PERGAMON

Chemical Engineering Science 56 (2001) 6143–6148

Chemical Engineering Science

www.elsevier.com/locate/ces

Gas hold-up and bubble diameters in a gassed oscillatory baffled column

M. S. N. Oliveira, X. Ni *

Department of Mechanical and Chemical Engineering, Centre for Oscillatory Baffled Reactor Applications (COBRA), Heriot-Watt University, Edinburgh EH14 4AS, Scotland, UK

Abstract

In this paper attempts are made to address how bubble behaviour in a batch oscillatory baffled column (OBC) contributes to the overall measured enhancement in mass transfer. A CCD camera is used to measure the bubble size distribution and the gas hold-up in the OBC. The experimental results of Sauter mean diameter and gas hold-up are correlated as a function of the power dissipation and superficial gas velocity, in order to allow for comparisons with published correlations for the mass transfer coefficient. In general, an increase in the oscillatory velocity causes an increase in the hold-up and a decrease in the Sauter mean diameter. Furthermore, we are able to show that the changes in the gas hold-up contribute more than the mean bubble size to the control of the mass transfer coefficient.

Keywords: Oscillatory baffled column; Bubble size distribution; Mean bubble size; Hold-up; Mass transfer

1. Introduction

Gas–liquid contact systems are widely employed in Chemical and Biological processes. Gas-sparged stirred tanks, bubble columns and airlift columns are the most commonly used devices for enhancing gas–liquid mass transfer. The oscillatory baffled column (OBC) is a relatively new mixing device and has recently been studied in gas–liquid applications (Hewgill, Mackley, Pandit, & Pannu, 1993; Ni, Gao, Cumming, & Pritchard, 1995). The OBC is based on the methodology of superimposing periodic fluid oscillations onto a cylindrical column containing evenly spaced orifice baffles. For batch operations, such a column is usually operated vertically. Fluid oscillation is achieved by means of a piston or bellows at the base of the column, or by moving a set of baffles up and down the column. The flow passing the baffles induces vortices, which provide intensive radial motion within the column. It is the strong radial velocity of similar magnitude to the axial velocity that gives uniform mixing in each inter-baffle zone and cumulatively along the length of the column (Brunold, Hunns, Mackley, & Thompson, 1989; Mackley & Ni, 1991, 1993). The fluid mechanical conditions in a batch OBC are governed by two dimensionless groups, i.e. oscillatory Reynolds (Re_o) and Strouhal number (St), defined as

$$Re_o = \frac{\omega x_o \rho D}{\mu}, \tag{1}$$

$$St = \frac{D}{4\pi x_o}, \tag{2}$$

where D is the column diameter (m), ρ the fluid density (kg m^{-3}), μ the fluid viscosity (kg m s^{-1}), x_o the oscillation amplitude (m), ω the angular frequency of oscillation ($=2\pi f$) and f the oscillation frequency (Hz). The oscillatory Reynolds number describes the intensity of mixing applied to the column, while the Strouhal number is the ratio of column diameter to stroke length, measuring the effective eddy propagation (Ni & Gough, 1997).

Using the quasi-steady approach proposed initially by Jealous & Johnson (1955) the time-averaged power density in an OBC can be estimated by

$$(P/V)_O = \frac{2\rho N_b}{3\pi C_D^2}\frac{1-\alpha^2}{\alpha^2}x_o^3\omega^3 \quad (\mathrm{W\ m^{-3}}), \tag{3}$$

where P/V is the time-averaged power density (W m^{-3}), N_b the number of baffles per unit length (m^{-1}), C_D the orifice discharge coefficient (taken as 0.7 for this type of constriction, Perry & Green, 1984), α the baffle free cross-sectional area defined as D_o/D and D_o the baffle

* Corresponding author. Tel.: +44-131-4513781; fax: +44-131-4513077.

E-mail address: x.ni@hw.ac.uk (X. Ni).

0009-2509/01/$ - see front matter
PII: S0009-2509(01)00257-3

orifice diameter (m). In addition to the external power supplied to the OBC, the specific power dissipation due to rising gas bubbles in a gas–liquid system should also be considered. This term was originally suggested by Calderbank, Evans, and Rennie (1960) as

$$(P/V)_B = U_g \rho g \quad (\mathrm{W\ m^{-3}}), \tag{4}$$

where U_g is the superficial gas velocity (m s^{-1}) and g is the gravitational constant (m s^{-2}). In gas–liquid systems the overall time-averaged power density is thus the sum of the two terms:

$$P/V = (P/V)_B + (P/V)_O. \tag{5}$$

The use of pulsation to enhance gas–liquid mass transfer has been reported previously, see for example, Baird and Garstang (1972), Baird and Rama Rao (1988), but only recently was this type of study extended to an OBC. The overall gas–liquid volumetric mass transfer coefficient, k_La, in an OBC was found to be six times higher than that in a bubble column (Hewgill et al., 1993) and 75% higher than that in a stirred tank fermenter involving a yeast culture (Ni et al., 1995). However, no attempt was made in these studies to identify which characteristics of the gas phase in the OBC provided such enhancements in the mass transfer rate. In an OBC, bubbles go through continuous breakage and coalescence processes along the column and stay in each baffled cell longer due to the motion of vortices as compared with a bubble column. We expect that both the bubble size and bubble mean residence time would contribute to the measured mass transfer enhancement. The mean residence time of the bubbles in the OBC can however be assumed to be proportional to the gas hold-up, ε_G. In this paper we report our experimental studies of bubble size distribution and gas hold-up in an OBC with the view of identifying mass transfer contributions.

2. Experimental facilities and procedure

2.1. Experimental apparatus

A schematic diagram of the apparatus is shown in Fig. 1. The OBC consists of a 50 mm internal diameter and 1.5 m tall Perspex column. The column was flanged vertically onto a metal table and supported by four rods in order to minimise external mechanical vibrations. The column was operated at room temperature with the top open to atmosphere and was filled with 2.5 l of tap water. A set of 14 orifice baffles was used with the baffles being made of 2 mm thick polyethylene plate and designed to fit closely to the wall of the column. The baffles were equally spaced at 75 mm apart (1.5 times the tube internal diameter) and supported by four 2 mm diameter stainless steel rods. The orifice diameter is 24 mm, giving a 23% free cross-sectional area. The liquid oscillation was achieved using a stainless steel bellows mounted at the base of the OBC and driven by an inverter connected to an electrical motor. The oscillation frequencies, from 1 to 5 Hz, can be controlled using a speed controller. The oscillation amplitudes, of 2–8 mm centre-to-peak, were obtained by adjusting the off-centre position of the connecting rod in the flying wheel. Air was continually supplied at the base of the column via a 1 mm nozzle. The airflow rate was controlled by a valve and measured by a calibrated rotameter. Aeration rates range from 0.05 to 0.3 vvm, where vvm is the volume of air per volume of liquid per minute. Table 1 shows the conversion between the aeration rates expressed in terms of vvm and the superficial gas velocities and Table 2 summarises the range of operational variables examined in this work. Flow visualisation was carried out using a CCD camera (Jai CV-M1) at two locations along the column as shown in Fig. 1; near the base of the column where the injection takes place and at approximately 650 mm away from the base of the column. The CCD camera has a resolution of 1000 × 1000 TV lines and a maximum shutter speed of 1/10000 s. The column sections for the flow visualisation were encased with a square viewing box filled with water to eliminate effects of wall curvature.

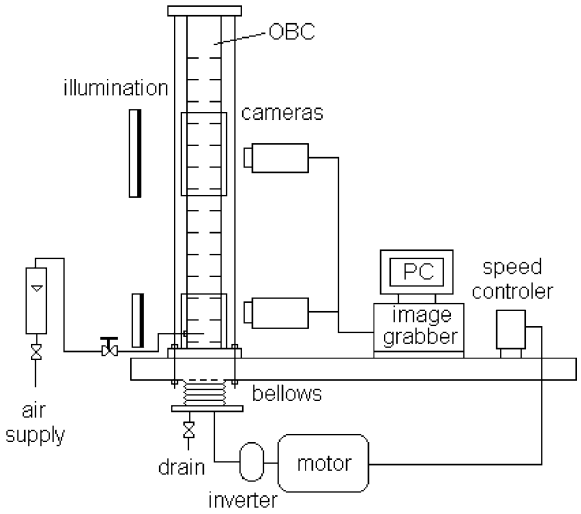

Fig. 1. Schematic diagram of the experimental apparatus.

Table 1
Conversion between aeration rate and superficial gas velocity

Aeration rate (vvm)	U_g (m s^{-1})
0.05	1.06×10^{-3}
0.1	2.12×10^{-3}
0.13	2.76×10^{-3}
0.2	4.24×10^{-3}
0.3	6.37×10^{-3}

Table 2
Range of operational variables examined

	Oscillation amplitude (mm)	Oscillation frequency (Hz)	Aeration rates (vvm)
Present study in d_{32}	2, 4, 8	1, 2, 3	0.05, 0.1, 0.2
Present study in ε_G	2, 4, 8	1, 2, 3, 4, 5	0.05, 0.1, 0.13, 0.2, 0.3
Ni and Gao (1996) in k_La	4, 8, 9, 12	3, 4, 5, 6, 7, 8	0, 0.25, 0.5, 0.75, 1

2.2. Bubble size distribution and mean bubble size

2.2.1. Procedure

Bubble images were obtained using the CCD camera operated at a shutter speed of 1/3000 s and placed at approximately 0.3 m away from the centre of the column. Back-illumination was provided by floodlights masked with a semi-transparent paper. The images were acquired using VidPIV 4.0 Rowan and processed using AEQUITAS-IA (version 1.3) image analysis software. By measuring bubbles' projected area, a_{proj}, the equivalent circular diameters, d_{eq} (diameter of a circle having the same area as the projected area of the bubble), were calculated according to

$$d_{\text{eq}} = \sqrt{\frac{4a_{\text{proj}}}{\pi}} \quad (\text{m}). \tag{6}$$

The bubble size distribution (BSD) curves are generated by the bubble number fraction vs. d_{eq} and the Sauter mean diameter, d_{32}, can also be calculated via

$$d_{32} = \frac{\sum (n_i \cdot d_{\text{eq}_i}^3)}{\sum (n_i \cdot d_{\text{eq}_i}^2)} \quad (\text{m}), \tag{7}$$

where n_i is the number of bubbles with size d_{eq_i}. Sample size and repeatability tests were carried out and a minimum of 300 bubbles were selected to obtain a representative BSD.

2.3. Gas hold-up

The gas hold-up was measured by recording the changes in the liquid height in the OBC using a CCD camera together with a fine scale fixed on the column. The procedure involves measuring the liquid level, h_0, at the top of the column without the presence of gas and the corresponding level, h, when gas is continuously introduced at a given flow rate. The hold-up is calculated from

$$\varepsilon_G = \frac{h - h_0}{h}. \tag{8}$$

3. Bubble size distribution and Sauter mean diameter

The application of oscillatory motion to a baffled column induces significant modifications in bubble trajectories, resulting in a complex liquid–bubble mixing pattern. This pattern is highly affected by the Re_o and St. At low oscillatory Reynolds numbers bubbles are seen to mainly move upwards, but as the level of oscillation is increased bubbles start to move downwards in certain phases of the oscillation cycle, exploring all the regions of the baffled-cells. At very intense levels of oscillation, rising bubbles are trapped within each cell for several seconds. The fluid oscillation in the presence of baffles also makes breakage and coalescence of bubbles become regular events in each baffled cell. The bubble size distribution profiles evidencing the frequency effect are captured in Fig. 2, where the bubble number fraction is defined as

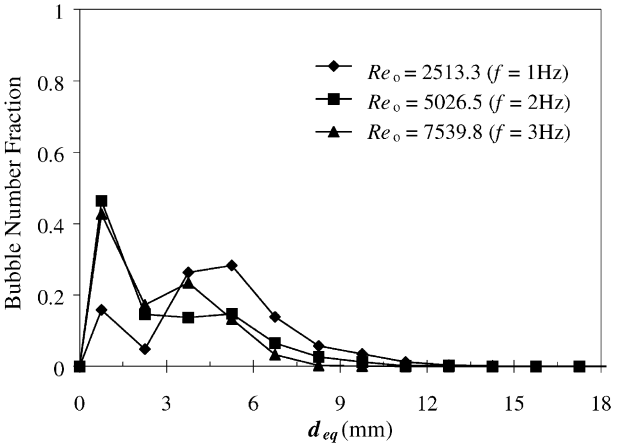

Fig. 2. Bubble size distribution. Baffles, oscillation ($x_o = 8$ mm), aeration rate = 0.05 vvm.

$$\text{Number fraction} = \frac{n_i}{\sum n_i}. \tag{9}$$

The increase in the oscillatory Reynolds number via the oscillation frequency gave narrower BSD and reduced the mean bubble size. This is expected as the increase in the oscillation velocity causes an increase in the power density to the system, subsequently resulting in smaller bubbles.

Fig. 3 shows the effect of the operating conditions on the Sauter mean bubble diameter, where d_{32} is plotted as a function of the oscillation Reynolds number, Re_o, for three aeration rates. For low oscillatory Reynolds numbers, oscillation has little effect on the mean diameter, and the superficial gas velocity is the dominating factor. This can be seen as the mean bubble size is higher at

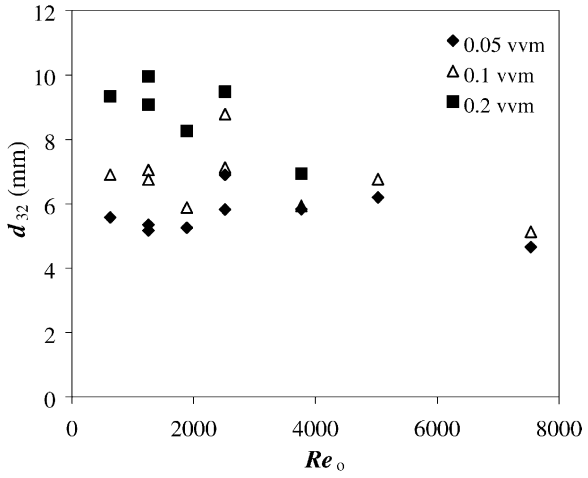

Fig. 3. Effect of oscillatory Reynolds number and aeration rate on d_{32}.

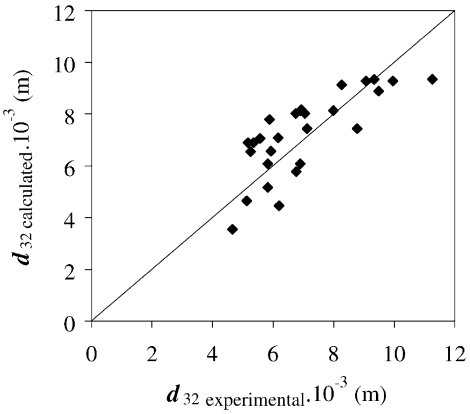

Fig. 4. Comparison of the experimental and the calculated d_{32}. The line drawn corresponds to the $x = y$ line.

higher aeration rates. The observations are within our expectations since, as the density of bubbles increases with the increase of U_g, more bubble coalescence is expected. For high oscillatory Reynolds numbers, more turbulence prevails within the OBC at increased power dissipation in the system, consequently the mean bubble diameter is significantly reduced. In these cases, the effect of superficial gas velocity is hindered and the oscillation becomes the dominating factor.

From the above discussion, it is clear that both the power density and aeration rate affect d_{32}. In analogy to the mass transfer coefficient, we anticipate that d_{32} will have a similar power law relationship with the time-averaged power density and the superficial gas velocity as

$$d_{32} = kU_g^m (P/V)^n, \tag{10}$$

where k, m and n are constants. By fitting the d_{32} results to the above equation, we have

$$d_{32} = 0.175 U_g^{0.4} (P/V)^{-0.2} \quad \text{(m)}. \tag{11}$$

The correlation indicates that on the control of d_{32} the superficial gas velocity plays a more significant role than the oscillation intensity. Fig. 4 compares the measured Sauter mean diameter values with those predicted using the correlation and the average and maximum relative errors were ±15% and ±33%, respectively.

4. Gas hold-up

The gas hold-up studies were carried out in the presence of both baffles and oscillation. The measurements of ε_G as a function of the oscillatory Reynolds number are plotted in Fig. 5. There are generally two patterns that can be observed: at low oscillatory Reynolds numbers the changes in hold-up are very small, but at high

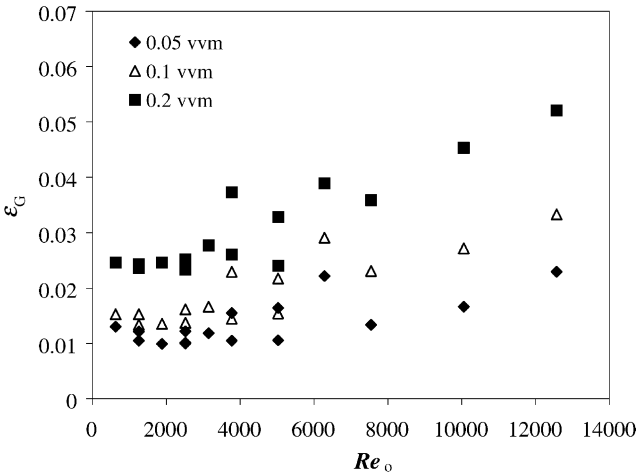

Fig. 5. Effect of oscillatory Reynolds number and aeration rate on ε_G.

oscillatory Reynolds numbers ε_G increases with the increased oscillation intensities. For the latter case, the oscillatory motion causes increased breakage, resulting in more of small and tiny bubbles from the experimental observations, hence longer residence times and higher hold-ups in the column. At a given oscillatory Reynolds number, the gas hold-up again increases with the increase of the aeration rate.

Once again, we assume the similar power law relationship between ε_G, U_g and P/V. By best fitting the hold-up data, we have

$$\varepsilon_G = 0.1 U_g^{0.4} (P/V)^{0.2}. \tag{12}$$

The correlation again confirms the dominant effect of the superficial gas velocity over the oscillation intensities. Fig. 6 compares the measured hold-up values with those predicted using Eq. (12), and the relative mean and maximum errors are ±13%, and ±55%, respectively.

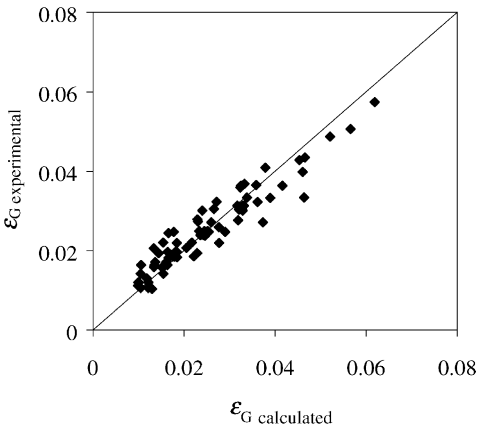

Fig. 6. Comparison of the experimental and the calculated gas hold-up. The line drawn corresponds to the $x = y$ line.

5. Mass transfer coefficient

Having established the correlations of d_{32} and ε_G with the superficial gas velocity and power density in the OBC, we can now determine the contributions of d_{32} and ε_G to k_La. To do that, we use, as the starting point, the correlation of k_La proposed by Ni and Gao (1996), as this was obtained using a similar geometric design and gas distributor. The correlation for k_La was reported as

$$k_La = 0.0256U_g^{0.37}(P/V)^{0.425} \quad (\mathrm{s}^{-1}) \tag{13}$$

for the operating conditions shown in Table 2. It should be noted that the definition of P/V used by Ni and Gao (1996) did not take into account the power due to aeration. However, their oscillation ranges were relatively high and under those conditions the power due to the oscillation was the dominating component. Consequently, the errors between the two power densities are relatively small. Combining Eqs. (11)–(13) together with dimensional analysis, we obtain the following:

$$k_La = 0.284\frac{\varepsilon_G^{1.5}}{d_{32}^{0.6}}. \tag{14}$$

This correlation shows that both bubble size and hold-up contribute to the k_La enhancement, with a significantly larger contribution from the gas hold-up. It is the combination of smaller bubbles with the tortuous routes for bubbles to travel (higher ε_G) that promotes the enhanced mass transfer.

6. Conclusions

In this paper, we have reported our extensive experimental measurements of bubble size distributions and gas hold-up in an OBC. The results have led us to identify the individual contribution of the bubble mean diameter and gas hold-up to the overall mass transfer coefficient. In the OBC, the changes in the gas hold-up play a more significant role than the changes in the mean diameter but it is the combination of smaller bubbles with longer residence times that resulted in the measured mass transfer enhancement.

Notation

a_{proj}	bubble projected area, m^2
BSD	bubble size distribution
C_D	orifice discharge coefficient
D	column diameter, m
D_o	baffle orifice diameter, m
d_{eq}	equivalent spherical bubble diameter, m
d_{32}	bubble Sauter mean diameter in the bulk of the column, m
f	oscillatory frequency, Hz
g	gravitational constant, $\mathrm{m\ s}^{-2}$
h	gas–liquid dispersion level, m
h_0	liquid height, m
k	constant (Eq. (10))
k_La	gas–liquid volumetric mass transfer coefficient, s^{-1}
m	constant (Eq. (10))
n	constant (Eq. (10))
N_b	number of baffles per unit length
OBC	oscillatory baffled column
P/V	time averaged power density, $\mathrm{W\ m}^{-3}$
Re_o	oscillatory Reynolds number
St	Strouhal number
U_g	superficial gas velocity, $\mathrm{m\ s}^{-1}$
vvm	volume of air per volume of liquid per minute
x_o	centre-to-peak amplitude of oscillation, m

Greek letters

α	baffle free cross-sectional area
ε_G	gas hold-up
μ	fluid viscosity, Pa s
ρ	liquid density, $\mathrm{kg\ m}^{-3}$
ω	radial frequency, $\mathrm{rad\ s}^{-1}$

References

Baird, M. H. I., & Garstang, J. H. (1972). Gas absorption in a pulsed bubble column. *Chemical Engineering Science*, *27*, 823–833.

Baird, M. H. I., & Rama Rao, N. V. (1988). Characteristics of a countercurrent reciprocating plate bubble column. II. Axial mixing and mass transfer. *Canadian Journal of Chemical Engineering*, *66*, 222–231.

Brunold, C. R., Hunns, J. C. B., Mackley, M. R., & Thompson, J. W. (1989). Experimental observations on flow patterns and energy losses for oscillatory flow in ducts containing sharp edges. *Chemical Engineering Science*, *44*, 1227–1244.

Calderbank, P. H., Evans, F., & Rennie, J. (1960). *Proceedings international symposium on distillation*, *Inst. Chem. Engrs. Brighton*.

Hewgill, M. R., Mackley, M. R., Pandit, A. B., & Pannu, S. S. (1993). Enhancement of gas–liquid mass transfer using oscillatory flow in a baffled tube. *Chemical Engineering Science*, *48*, 799–809.

Jealous, A. C., & Johnson, H. F. (1955). Power requirements for pulse generation in pulse columns. *Industrial and Engineering Chemistry*, *47*(6), 1159–1166.

Mackley, M. R., & Ni, X. (1991). Mixing and dispersion in a baffled tube for steady laminar and pulsatile flow. *Chemical Engineering Science*, *46*, 3139–3151.

Mackley, M. R., & Ni, X. (1993). Experimental fluid dispersion measurements in periodic baffled tube arrays. *Chemical Engineering Science*, *48*, 3293–3305.

Ni, X., & Gao, S. (1996). Scale-up correlation for mass transfer coefficients in pulsed baffled reactors. *Chemical Engineering Journal*, *63*, 157–166.

Ni, X., & Gough, P. (1997). On the discussion of the dimensionless groups governing oscillatory flow in a baffled tube. *Chemical Engineering Science*, *52*, 3209–3212.

Ni, X., Gao, S., Cumming, R. H., & Pritchard, D. W. (1995). A comparative study of mass transfer in yeast for a batch pulsed baffled bioreactor and a stirred tank fermenter. *Chemical Engineering Science*, *50*, 2127–2136.

Perry, R. H., & Green, D. (1984). *Perry's chemical engineers' handbook* (6th ed.). New York: McGraw Hill.